



HAL
open science

Flame Retardancy of PA6 Using a Guanidine Sulfamate/Melamine Polyphosphate Mixture

Mathieu Coquelle, Sophie Duquesne, Mathilde Casetta, J Sun, Xiaoyu Gu, Sheng Zhang, Serge Bourbigot

► **To cite this version:**

Mathieu Coquelle, Sophie Duquesne, Mathilde Casetta, J Sun, Xiaoyu Gu, et al.. Flame Retardancy of PA6 Using a Guanidine Sulfamate/Melamine Polyphosphate Mixture. *Polymers*, 2015, *Polymers*, 7 (2), pp.316-332. 10.3390/polym7020316 . hal-03944878

HAL Id: hal-03944878

<https://hal.univ-lille.fr/hal-03944878v1>

Submitted on 18 Jan 2023

HAL is a multi-disciplinary open access archive for the deposit and dissemination of scientific research documents, whether they are published or not. The documents may come from teaching and research institutions in France or abroad, or from public or private research centers.

L'archive ouverte pluridisciplinaire **HAL**, est destinée au dépôt et à la diffusion de documents scientifiques de niveau recherche, publiés ou non, émanant des établissements d'enseignement et de recherche français ou étrangers, des laboratoires publics ou privés.



Distributed under a Creative Commons Attribution 4.0 International License

Article

Flame Retardancy of PA6 Using a Guanidine Sulfamate/Melamine Polyphosphate Mixture

Mathieu Coquelle ¹, Sophie Duquesne ^{1,*}, Mathilde Casetta ¹, Jun Sun ², Xiaoyu Gu ², Sheng Zhang ² and Serge Bourbigot ¹

¹ R₂Fire/UMET—UMR/CNRS 8207, Ecole Nationale Supérieure de Chimie de Lille (ENSCL), CS 90108, 59652 Villeneuve d'Ascq Cedex, France; E-Mails: mcoquelle@enscl.fr (M.C.); mathilde.casetta@univ-lille1.fr (M.C.); serge.bourbigot@enscl-lille.fr (S.B.)

² Key Laboratory of Carbon Fiber and Functional Polymers, Beijing University of Chemical Technology, Ministry of Education, Beijing 100029, China; E-Mails: sunjunbuct@gmail.com (J.S.); guxy@mail.buct.edu.cn (X.G.); szhang1966@163.com (S.Z.)

* Author to whom correspondence should be addressed; E-Mail: sophie.duquesne@enscl-lille.fr; Tel.: +33-3-2033-7236.

Academic Editors: Alexander Morgan and A. Richard Horrocks

Received: 28 November 2014 / Accepted: 4 February 2015 / Published: 13 February 2015

Abstract: Polyamide 6 (PA6) is a widely-used polymer that could find applications in various sectors, including home textiles, transportation or construction. However, due to its organic nature, PA6 is flammable, and flame-retardant formulations have to be developed to comply with fire safety standards. Recently, it was proposed to use ammonium sulfamate as an effective flame retardant for PA6, even at low loading content. However, processing issues could occur with this additive considering large-scale production. This paper thus studies the use of another sulfamate salt—guanidine sulfamate (GAS)—and evidences its high efficiency when combined with melamine polyphosphate (MPP) as a flame retardant for PA6. A decrease of the peak of the heat release rate by 30% compared to pure PA6 was obtained using only 5 wt% of a GAS/MPP mixture in a microscale calorimeter. Moreover, PA6 containing the mixture GAS/MPP exhibits a Limiting Oxygen Index (LOI) of 37 vol% and is rated V0 for the UL 94 test (Vertical Burning Test; ASTM D 3801). The mechanisms of degradation were investigated analyzing the gas phase and solid phase when the material degrades. It was proposed that MPP and GAS modify the degradation pathway of PA6, leading to the formation of nitrile end-group-containing molecules. Moreover, the formation of a polyaromatic structure by the reaction of MPP and PA6 was also shown.

Keywords: polyamide 6; guanidine sulfamate; flame retardancy

1. Introduction

The organic nature of polymers, like polyamide 6 (PA6), is an issue in terms of flammability for certain applications. That is the reason why materials have to comply with strict fire safety requirements in applications, such as transport, electrical and electronic parts, for example. In order to comply with these requirements, fire retardants (FR) are usually added to the polymer when melted during extrusion.

The use of ammonium sulfamate (AS) has been described as an effective FR for PA6 in previous studies [1,2]. It was shown that this compound was active at very low loadings (<5 wt%). More recently, ammonium sulfamate was effectively added to PA6 fibers to improve their fire behavior; however, it was shown that the FR loadings and processing parameters might be issues regarding the matrix degradation, because of the high temperature usually involved in PA6 processing [3]. This was attributed to the release of ammonia from AS, leading to aminolysis of the PA6 during processing. This could limit the use of AS as a flame retardant for PA6 at an industrial scale.

In order to limit the risks of matrix degradation, it is proposed in this work to substitute AS by guanidine sulfamate (GAS). Indeed, guanidine sulfamate is already reported as a flame retardant agent in PVC and in PA6 [4]. Moreover, to improve its efficiency, it is proposed to combine it with other flame retardants. It is reported in the literature that sulfur compounds can act as synergists with phosphorus based compounds such as ammonium polyphosphate [5], but the literature on this subject is very limited. Ammonium polyphosphate (APP) is widely used, in particular in intumescent systems, as an acid source. High amounts of APP (generally >20 wt%) are usually needed to efficiently flame retard PA6 [6]. Moreover, APP has a relatively low thermal stability and requires fast processing to avoid its degradation when used in PA6 [7]. That is the reason why melamine polyphosphate (MPP) was considered in this work, since it is thermally stable at the processing temperature of PA6. Moreover, MPP is already widely used in the fire retardancy of polyamides and has applications in PA6 and glass fiber-reinforced PA6 and PA6 with a UL 94 V0 rating (Vertical Burning Test; ASTM D 3801) [8] has been claimed using melamine in combination with guanidine sulfamate [4]. MPP is also an excellent co-additive with other phosphorus-based compounds, enhancing the fire performance and limiting the degradation of polyamide during processing. MPP will thus be used as a potential co-flame retardant with guanidine sulfamate in this study.

In this context, the first part of this paper aims at investigating, at the lab scale, the influence of the GAS/MPP ratio on the fire performance of PA6/GAS/MPP evaluated according to micro-scale combustion calorimetry (MCC). In the second part, the most effective formulation will be processed at a large scale, and its fire performance will be evaluated using various testing methods. The last part of this paper will be dedicated to the investigation of the mechanism of degradation of PA6/GAS/MPP, analyzing both the condensed and gaseous degradation products when the materials are exposed to high temperature.

2. Experimental

2.1. Materials

PA6 was supplied by Solvay (Brussels, Belgium) under the trade name, Technyl S27 BL. The FR additives are guanidine sulfamate (GAS) supplied by Jinchi Chemicals Co. (Zunhua, China) and melamine polyphosphate (MPP, Melapur[®] 200) supplied by BASF (Ludwigshafen, Germany). PA6, MPP and GAS were dried at 80 °C for at least 24 h before use.

2.2. Preparation of Samples

Different formulations PA6/GAS/MPP (Table 1) were prepared by microextrusion using a DSM Xplore micro 15 device (Xplore Instruments, Geleen, The Netherlands) having a volume of 15 cm³. The total amount of additives was fixed at 5 wt%, and the ratio between GAS and MPP varied. The PA6 matrix (pellets) and additives were extruded under a nitrogen flow at 245 °C and 100 rpm for 3 min.

Table 1. Polyamide 6 (PA6)/guanidine sulfamate (GAS)/melamine polyphosphate (MPP) formulations.

| Materials | PA6 wt% | GAS wt% | MPP wt% |
|-----------------------|---------|---------|---------|
| PA6 | 100 | 0 | 0 |
| PA6/MPP 5% | 95 | 0 | 5 |
| PA6/GAS 1%/MPP 4% | 95 | 1 | 4 |
| PA6/GAS 2.5%/MPP 2.5% | 95 | 2.5 | 2.5 |
| PA6/GAS 4%/MPP 1% | 95 | 4 | 1 |
| PA6/GAS 5% | 95 | 5 | 0 |

Large-scale extrusions were performed on a Thermo Scientific HAAKE PolyLab OS System (Waltham, MA, USA) under nitrogen. It consists of a twin-screw laboratory extruder equipped with feed-dosing elements. The temperature profile of the 10 heating elements was set as reported in Table 2. Formulations were then pelletized to be compression molded into samples, whose size is defined according to the standards required for the fire tests.

Table 2. Temperature profile of the extruder from hopper to die.

| Zone | 1 * | 2 | 3 | 4 | 5 ** | 6 | 7 | 8 | 9 | 10 |
|------------------|-----|-----|-----|-----|------|-----|-----|-----|-----|-----|
| Temperature (°C) | 300 | 280 | 260 | 260 | 240 | 240 | 235 | 230 | 230 | 210 |

* PA6 was fed in Zone 1; ** fire retardants (FR) were fed in Zone 5.

2.3. Fire Testing Methods

Micro-scale combustion calorimetry (MCC) FAA Micro Calorimeter, Fire Testing Technology, East Grinstead, UK) was used to assess the flammability of the formulations. Tests were performed according to ASTM D-7309 [9] at a heating rate of 1 °C/s, a maximum pyrolysis temperature of 750 °C and a combustion temperature of 900 °C. The flow was a mixture of O₂/N₂ 20/80 cm³·min⁻¹, and the sample weight was 6.3 ± 0.1 mg. All experiments were performed in triplicate, and heat release rate (HRR) values are reproducible to within ±5%.

Mass loss calorimetry (MLC) (Mass Loss Calorimeter, Fire Testing Technology) was performed according to the ISO 13927 procedure [10]. A flat horizontal sample ($100 \times 100 \times 3 \text{ mm}^3$) located at 25 mm below the radiant conical heater of the MLC was exposed to a radiative heat flux of $35 \text{ kW} \cdot \text{m}^{-2}$ to simulate a mild fire. Ignition is provided by an intermittent spark igniter located 13 mm above the sample. From this experiment, time to ignition (TTI), heat release rate (HRR) and total heat release (THR) were obtained. Methane was used as the calibration gas.

The Limiting Oxygen Index (LOI) was measured according to the standard [11] using a Fire Testing Technology instrument. This allows determining the minimum concentration of oxygen (in vol%) in a nitrogen/oxygen mixture that is required for the combustion of a material in vertical position ignited at the top. LOI was measured on samples of $100 \times 10 \times 3 \text{ mm}^3$, and the values are repeatable within $\pm 1 \text{ vol}\%$.

UL 94 tests were performed on a Fire Testing Technology equipment using barrels of $127 \times 12.7 \times 1.6 \text{ mm}^3$, in accordance with the recommendations of the standard [8]. The barrels are ignited by a blue flame (without cone) of 20 mm. The burner that generates the flame is supplied with methane gas having a flow rate of 105 mL/min with a back pressure lower than 10 mm of water. For each formulation, five specimens are tested after a preconditioning at $23 \pm 2 \text{ }^\circ\text{C}$ for a minimum of 48 h.

2.4. Thermogravimetric Analysis

Thermogravimetric analysis (TGA) was performed using a TA Instruments Q5000 (New Castle, DE, USA) with a balance purge flow of 10 mL/min (nitrogen), a heating ramp of $10 \text{ }^\circ\text{C}/\text{min}$ from 50 to $800 \text{ }^\circ\text{C}$ and a sample purge flow of 100 mL/min under air. For each experiment, 10 mg of the materials (powder) were placed into open alumina pans.

2.5. Analysis of the Decomposition Gases

Decomposition gases were identified, coupling Fourier Transform Infrared Spectroscopy (FTIR) (Nicolet iS10, ThermoScientific, Madison, WI, USA) to TGA (the same TGA as described above). A transfer line with an inner diameter of 1 mm was used to connect the TGA and the infrared cell. Both the transfer line and the gas cell were heated at $225 \text{ }^\circ\text{C}$ to avoid the condensation of the decomposition products. The spectra were recorded between 400 and 4000 cm^{-1} , with the accumulation of 8 scans and an optical resolution of 4 cm^{-1} . For each test, 10 mg of the materials (powder) were placed into alumina pans.

2.6. Analysis of the Condensed Phase

TGA curves allow the determination of characteristic temperatures of the main degradation steps of the samples: $20 \text{ }^\circ\text{C}$, *i.e.*, before the degradation of the formulations; $275 \text{ }^\circ\text{C}$, corresponding to the beginning of the first degradation step of the PA6/GAS/MPP blend; $320 \text{ }^\circ\text{C}$, corresponding to the end of this first step; $410 \text{ }^\circ\text{C}$, during the main degradation step of the sample; and finally, $490 \text{ }^\circ\text{C}$, during the oxidation step. Thus, heat treatments were performed in a tubular furnace under air at those characteristic temperatures. For each sample, a heating rate of $10 \text{ }^\circ\text{C} \cdot \text{min}^{-1}$ was applied from room temperature to the selected temperature, followed by an isotherm of 1 h. The residues were then collected, ground and stored in a desiccator before analyzing them by solid-state nuclear magnetic resonance (NMR).

^{13}C solid-state NMR was performed using a Bruker Avance spectrometer (Billerica, MA, USA) and a 4-mm probe, working at 100.6 MHz (9.4 T) with cross-polarization (CP) ^1H - ^{13}C and dipolar decoupling (DD) with magic angle spinning (MAS) (spinning frequency of 10 kHz). The Hartmann–Hahn relation matching condition was obtained by adjusting the power on the ^1H channel for a maximum ^{13}C FID (Free Induction Decay) signal of glycine. All spectra were acquired with a contact time of 1 ms, and the delay between the pulses was 5 s. They were accumulated with a number of scans, varying from 1024 up to 50,000, to get an acceptable signal-to-noise ratio. Tetramethylsilane (TMS) was used as a reference.

^{31}P NMR measurements were performed on a Bruker Avance II spectrometer, working at 161.9 MHz (9.4 T) and at a spinning rate of 10 kHz. Bruker probe heads equipped with a 4-mm MAS assembly were used. Experiments were carried out using CP because of the long relaxation time of the phosphorus nuclei (10 to 500 s) with ^1H high-power dipolar decoupling (HPDEC). A recycle delay of 30 s was optimized and was applied for all samples. H_3PO_4 in aqueous solution (85%) was used as a reference for 0 ppm.

3. Results and Discussion

3.1. Preliminary Investigation of the MPP/GAS Combination

MCC curves of the formulations containing various ratios of GAS and MPP are presented in Figure 1, and Table 3 summarizes the MCC results for the formulations containing guanidine sulfamate or/and MPP.

The substitution of GAS by MPP leads to an improved fire behavior of PA6/GAS, in particular when 1 or 2.5 wt% of GAS are substituted. Reductions by 27% and 30% of the pHRR (peak of Heat Release Rate) are observed, respectively. However, when a higher amount of MPP is added to the formulation (4 wt%), the pHRR is the same as for the formulation containing 5 wt% GAS. On the other hand, the THR is only slowly affected by the substitution of GAS by MPP, and the differences between the samples remain in the range of the error. For all of the formulations containing MPP, a shift of the pHRR to a lower temperature (-50 to -70 °C) is observed, compared to neat PA6 and PA6/GAS 5%. The temperature at the pHRR is highly decreased when 4 wt% of GAS are substituted by MPP in the PA6/GAS formulation (450 to 390 °C). With the formulations containing 1 wt% and 2.5 wt% of MPP, the decrease is lower (between 20 and 30 °C). This suggests that MPP in the formulations favors the PA6 degradation. This will be further investigated later in this paper.

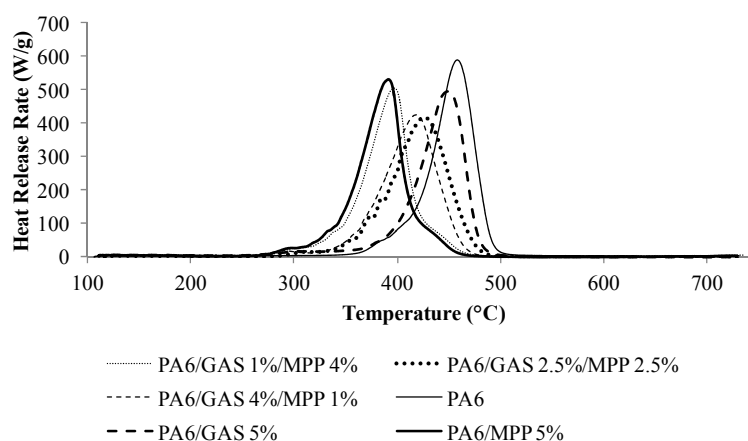


Figure 1. Heat release rate (HRR) curves vs. temperature obtained with pyrolysis combustion flow calorimetry (MCC) of PA6 and PA6/GAS/MPP formulations.

Table 3. MCC results of PA6, PA6/GAS 5% and PA6/GAS/MPP formulations. THR, total heat release.

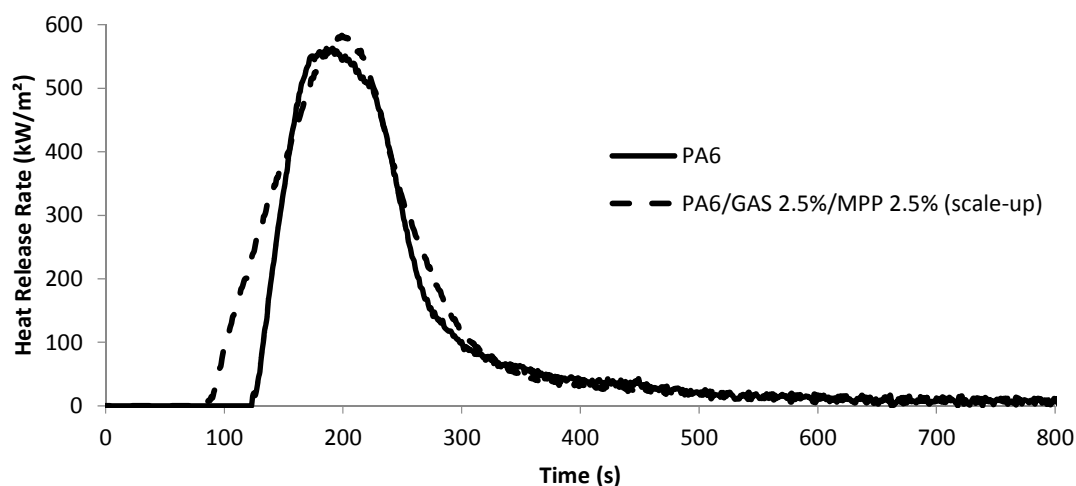
| Formulation | pHRR (W/g) | Δ pHRR/PA6 (%) | T_{pHRR} (°C) | THR (kJ/g) | Δ THR/PA6 (%) |
|-----------------------|------------|-----------------------|------------------------|------------|----------------------|
| PA6 | 588 | – | 456 | 30.0 | – |
| PA6/MPP 5% | 530 | –10 | 391 | 29.7 | –1.0 |
| PA6/GAS 1%/MPP 4% | 498 | –15 | 395 | 28.1 | –6.3 |
| PA6/GAS 2.5%/MPP 2.5% | 411 | –30 | 428 | 28.7 | –4.3 |
| PA6/GAS 4%/MPP 1% | 429 | –27 | 420 | 28.1 | –6.3 |
| PA6/GAS 5% | 500 | –15 | 449 | 27.4 | –8.7 |

Those results demonstrate that the ratio of 50/50 for GAS/MPP is found to be the most efficient to decrease the pHRR, and this formulation was thus selected for up-scaling. The formulation including 2.5% of GAS and 2.5% of MPP was thus extruded at the pilot scale, and its FR properties were determined using various fire testing methods.

3.2. Fire Retardant Properties of the PA6/GAS 2.5%/MPP 2.5%

3.2.1. Cone Calorimetry

The reaction to fire of the best formulation was first evaluated by mass-loss calorimetry and compared to pure PA6. HRR vs. time of the neat PA6 and of the fire-retarded formulation are presented in Figure 2. Characteristic data determined from the curves are summarized in Table 4.

**Figure 2.** Cone calorimetry curves of PA6 and the PA6/GAS 2.5%/MPP 2.5% formulation extruded at a large scale (35 kW/m², 25 mm).**Table 4.** Cone calorimetry data of PA6 and the PA6/GAS 2.5%/MPP 2.5% formulation extruded at a large scale (35 kW/m², 25 mm). TTI, time to ignition.

| Property | PA6 | PA6/GAS 2.5%/MPP 2.5% | Δ /PA6 (%) |
|---|----------|-----------------------|-------------------|
| peak HRR (kW/m ²) | 603 ± 13 | 582 ± 20 | –4 |
| time peak HRR (s) | 218 ± 16 | 213 ± 9 | –2 |
| TTI (s) | 124 ± 13 | 87 ± 2 | –30 |
| Total heat release (MJ/m ²) | 73 ± 2 | 79 ± 1 | +8 |

Similar values for pHRR, time to pHRR and THR are obtained for PA6 and flame-retarded PA6 taking into account the margin of error (10%). The calculated standard deviation indicates the good repeatability of the experiments, and the results concerning neat PA6 are similar to those already reported in the literature [12]; thus, we are confident with the obtained data. However, the obtained results may be surprising, since it was previously demonstrated that pHRR measured in the MCC was decreased by around 30% compared with PA6. However, it is noteworthy that the way the HRR is measured in both methods is different, as well as the fire scenario and the sample size. Indeed, whereas MCC is a mg-scale test method and fails to account for the physical effects that typically occur on larger length or mass scales, such as dripping or intumescence [13], this is not the case for mass loss calorimeter, and different behaviors are often reported between those two testing methods [14]. Moreover, Lewin *et al.* previously reported that when AS/dipentaerythritol are added at a loading respectively equal to 2 and 0.7 wt% in PA6, an increase in the pHRR from 1932 to 2408 kW/m² was observed [15]. This effect was attributed to the sulfate moieties' pyrolysis. It was proposed that sulfuric acid, formed when the sulfated polymer and polyol (formed from the sulfation reaction of the primary amino group of polyamide 6 (Equation (1)) and of the hydroxyl groups of dipentaerythritol (Equation (2))) decompose, reacts very rapidly with the polymer, leading to high HRRs:



On the other hand, the time to ignition (TTI) is significantly decreased when comparing the FR formulation with the neat PA6. In the test conditions (heat flux: 35 kW/m²; distance: 25 mm), neat PA6 has a TTI of 124 ± 13 s, whereas PA6/GAS 2.5%/MPP 2.5% has a TTI of 87 ± 2 s. This behavior could be brought to the thermal stability of the flame-retarded material, which is lower than that of pure PA6. Indeed, it could be reasonably proposed that the time to ignition is decreased because PA6 degradation is promoted in the presence of GAS and MPP, as observed with MCC. This will be further discussed in the paper.

On the other hand, it is noteworthy that the burning behavior during the MLC experiment is different comparing PA6 and the PA6/GAS 2.5%/MPP 2.5%. First, for both cases, it is observed that the materials first melt with bubbling, and the surface of the sample carbonizes; a thin carbonaceous skin is formed at the top of the bubbling surface. When this skin layer breaks, the fuel is released, and ignition occurs. The HRR increases at that time to reach a maximum at around 200 s. When the HRR starts to decrease and only in the case of the FR PA6, a new charred surface gradually appears and swells, leading to the formation of an intumescent structure at around 250 s, which is stable up to the end of the experiment (Figure 3). It could thus be reasonably assumed that, even if an intumescent structure is formed when GAS and MPP are combined in PA6, its kinetics of formation is too low to be effective.

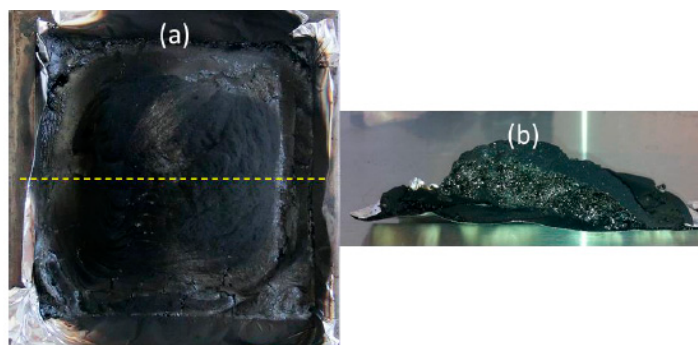


Figure 3. Cone calorimetry residues of PA6/GAS 2.5%/MPP 2.5% viewed from above (yellow line: cross-section) (a), and the view of the char cut in the cross-section (b).

3.2.2. UL 94 and LOI

LOI and the UL 94 rating were also determined for the material resulting from the pilot-scale process.

An LOI value of 28 vol% was obtained for neat PA6. Some high LOI values were already reported for neat PA6 [16,17] and were attributed to the melting behavior of PA6. This behavior is confirmed in this study, and it was observed that PA6 self-extinguished by moderate dripping (Figure 4a). Moreover, visual observation shows that the drips looked rather viscous. The FR formulation (PA6/GAS 2.5%/MPP 2.5%) exhibits an LOI of 37 vol% and was hardly ignited between 23 and 30 vol% of O₂ (Figure 4b). In this case, the small flame extinguishes by moderate dripping. On the other hand, when the oxygen content was raised to 31 up to 36 vol%, heavy dripping occurred, as shown in Figure 4c, removing the flame. In that case, drips present a lower viscosity (visual observation), as they flowed rapidly until the bottom of the barrel.



Figure 4. PA6 sample tested at an Oxygen Index (OI) below 28 vol% (a); the PA6/GAS 2.5%/MPP 2.5% sample tested at OI between 23 and 30 vol% (b) and between 31 and 36 vol% (c).

By visual observation of the burning behavior of the samples during the LOI test, it could be assumed that MPP and AS change the melt viscosity of PA6. Thanks to a lower viscosity, heavy dripping could remove material from the flaming zone and allow a quick extinction, leading to a high LOI value. This behavior was already observed by Levchik *et al.* [18] in PA6 containing melamine, melamine oxalate, melamine phthalate and melamine cyanurate.

UL 94 tests were performed to characterize the burning behavior of PA6 and PA6/GAS 2.5%/MPP 2.5%. Detailed results are reported in Table 5. It is observed that PA6 burns easily, but quickly flames out by dripping. The cotton is ignited for all samples, and the second ignition is shorter than the first. PA6 is thus rated V2. For the fire-retarded PA6, samples are easily ignited, and they extinguish, by dripping, more rapidly than neat PA6. For these samples, the cotton remains unburned after each test. PA6/GAS 2.5%/MPP 2.5% is thus rated V0.

Table 5. UL 94 results for neat PA6 and for PA6/GAS 2.5%/MPP 2.5% extruded at a large scale.

| Formulation | t_1/t_2 * (s) | Dripping ** | Cotton ignition ** | rating |
|-----------------------|-----------------|-------------|--------------------|--------|
| PA6 | 3.6/2.4 | Y | Y | V2 |
| PA6/GAS 2.5%/MPP 2.5% | 1.6/1.9 | Y | N | V0 |

* t_1 and t_2 , average combustion times after the first and the second application of the flame. ** Y: yes; N: no.

As previously described, considering the LOI tests, when pure PA6 burns, it leads to the formation of a melted material that presents a potentially higher viscosity than in presence of the GAS/MPP mixture. This behavior could be attributed to the effect of the FR additives, which would promote PA6 degradation. In fact, after ignition of the neat PA6, a large flaming droplet falls and ignites the cotton. Generally, one or two other droplets extinguished the materials by removing the flame from the burning sample. Concerning the FR PA6, the flame of the burning sample is removed by the first droplet. This small droplet is then extinguished during its fall and does not ignite the cotton. It is thus assumed that the difference in viscosity changes the size of the burning droplets, and large burning drops are not easily extinguished during the fall, whereas small droplets are. Kandola *et al.* have investigated the melt dripping of thermoplastic polymers [19]. They showed that, increasing the PA6 temperature, from 425 to 630 °C, produces drops with decreasing mass and diameter. Moreover, viscosity is a function of both temperature and molecular weight. If the FR additives promote PA6 degradation, shortened chains of low viscosity will be preferably formed during the degradation of the polymer, which at the end, leads to the formation of smaller drops that are easily extinguished. Further investigation using instrumented UL 94 tests [20] is currently being carried out in the lab to quantify this dripping.

The investigations carried out on the pilot-scale processed material thus demonstrated that using the GAS/MPP mixture in PA6 leads to improved fire retardant properties considering the LOI and UL 94 rating. Moreover, it was suggested that those FR additives will affect the thermal stability of the PA6 matrix, since both the TTI and the temperature at the maximum HRR measured on the MCC are decreased, comparing the FR PA6 with the virgin PA6. Thus, the next part of the paper will investigate the degradation mechanisms of PA6/GAS/MPP, analyzing first the gaseous degradation products released when the material is exposed to an increasing temperature.

3.3. Mechanism of Degradation of PA6/GAS/MPP

TGA-FTIR

Figure 5 presents the TG and DTG (Derivative ThermoGravimetric) curves of PA6 and the PA6/GAS 5% and PA6/GAS 2.5%/MPP 2.5% formulations obtained under air. A three-step decomposition is observed for neat PA6. From ambient temperature to 320 °C, a small weight loss of

2% is attributed to moisture release. The main step of degradation (between 320 and 480 °C with a maximum rate at 449 °C) corresponds to an 88% weight loss. The last step, from 480 to 540 °C, corresponds to a 10% weight loss and could be attributed to the oxidation of the transient residue. The main decomposition step corresponds to the volatilization of monomer and chain fragments, as reviewed in the literature [7,21].

For the formulations containing GAS/MPP or GAS, the first decomposition step occurs between around 270 °C and 320 °C, while no decomposition step was observed in that range of temperature for pure PA6. On the other hand, the main degradation step is observed at 420 °C for the GAS/MPP-containing formulation and at 450 °C for the PA6/GAS system. As a consequence, the main decomposition step occurs at a lower temperature when MPP is used in the formulation. This result confirms what has been previously observed, and it is thus reasonable to conclude that MPP promotes the degradation of PA6 in the first step. The last degradation step, attributed to the oxidation of the transient residue, is, however, observed at a higher temperature for both FR formulations. It could thus be concluded that the transient char formed when PA6 is flame retarded is less sensitive to oxidation compared to the one obtained in the case of virgin PA6.

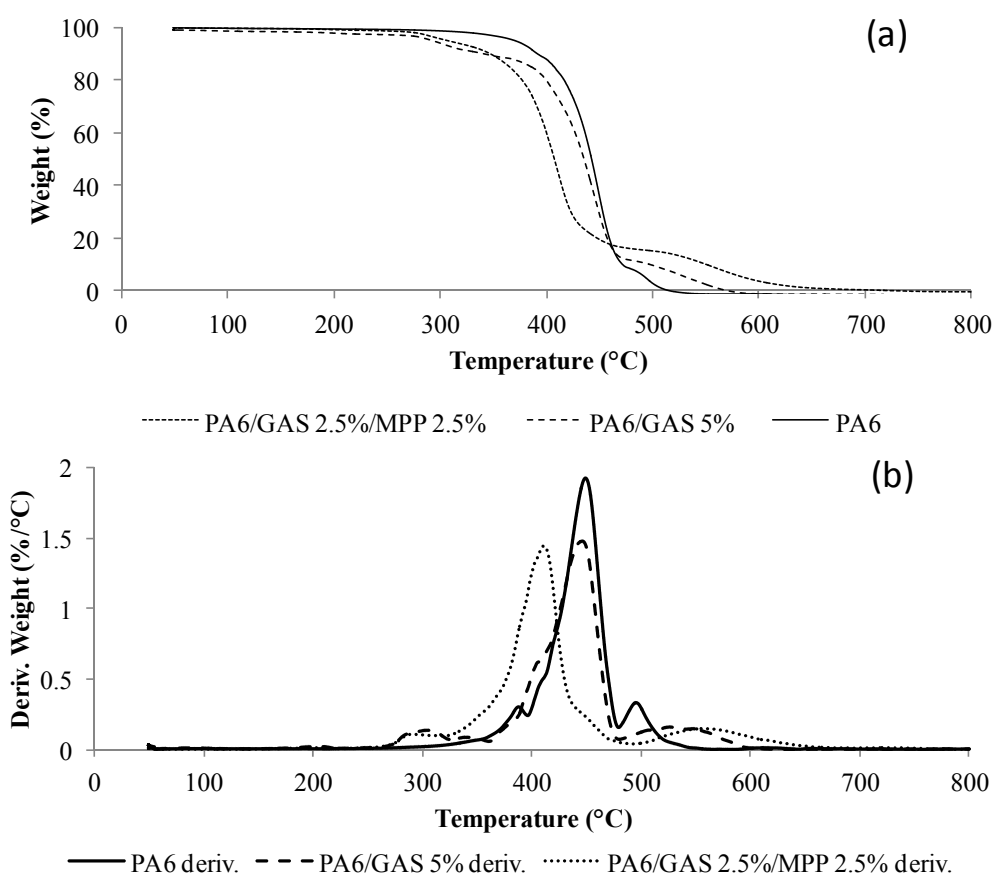


Figure 5. TG (a) and DTG curves (b) of PA6, and PA6/GAS 5% and PA6/2.5%/MPP 2.5% formulations (10 °C/min, air). Deriv. corresponds to derivative.

The gases evolved during the degradation of the materials were then analyzed using FTIR. The spectra of the gases collected during the thermo-oxidative degradation of the PA6/GAS formulations are presented in Figure 6, whereas Table 6 shows the full assignment of the peaks of the different

spectra [22–26]. The presented spectra are those that have been collected at the characteristic temperatures of degradation of the material previously determined according to the TG analyses. Three hundred degrees Celsius corresponds to the maximum weight loss rate of the first degradation step; 430 °C correspond to a temperature located in the zone where the degradation is maximum; and 500 °C corresponds to the oxidation of the transient residues. Spectra for both FR formulations show the same peaks for each temperature.

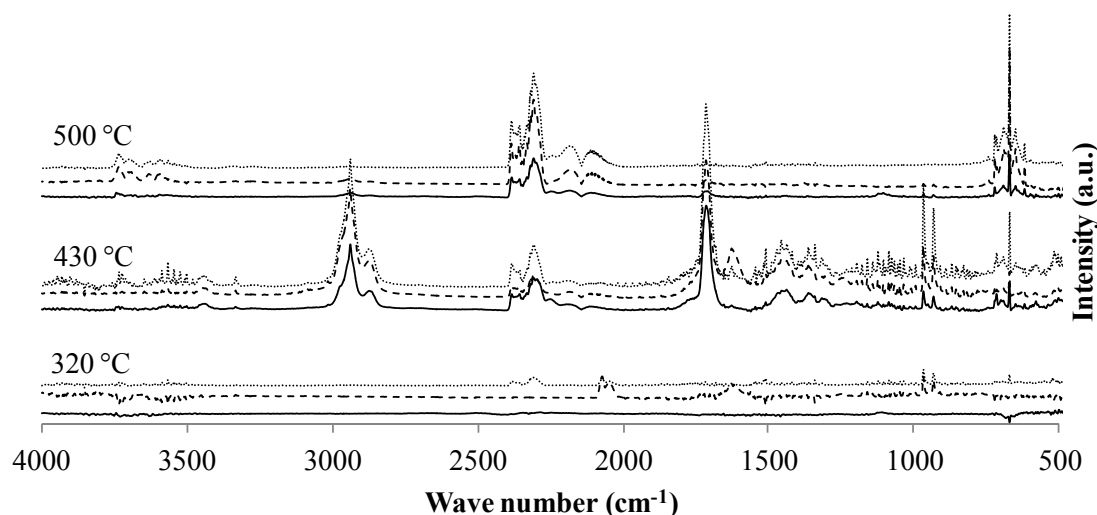


Figure 6. FTIR spectra of the gases evolved during the thermo-oxidative degradation of PA6 (—), PA6/GAS 5% (--) and PA6/GAS 2.5%/MPP 2.5% (···) at characteristic temperatures of degradation.

Table 6. IR peak assignments for PA6 and PA6/AS 5% (* primary, ** secondary).

| Functional Group or Component | Wave Number (cm ⁻¹) | Vibration Type | Additional Ref. |
|-------------------------------|---------------------------------|-----------------|-----------------|
| CO ₂ | 669 | δ | [22] |
| | 2354 | v _{as} | |
| NH ₃ | 930 | δ | [22,26] |
| | 965 | δ | |
| | 1626 | v | |
| | 3332 | v | |
| CH ₂ | 2873 | δ | [22] |
| | 2938 | δ | |
| N-CH ₂ | 1440 | δ | [22] |
| Amide I (prim. *, sec. **) | 1713 | v | [22,23] |
| Amide II (sec. **) | 1508 | δ, v | [22,23] |
| Amide III (prim. *) | 1340 | δ, v | [22,23] |
| -C≡N | 2250 | v | [22,25] |
| H ₂ O | 1400–1700 | δ | [22] |
| | 3400–3700 | v _{as} | |

In the case of PA6, the spectra collected at the first degradation step present only peaks attributed to water (3600 cm⁻¹ and 1500 cm⁻¹). Those peaks are observed during the whole experiment, since water is formed during the degradation of PA6 [1,21]. Around 430 °C, the main degradation product is

ϵ -caprolactam, exhibiting characteristic peaks at 2938 and 1713 cm^{-1} , corresponding respectively to the δ vibration of CH_2 groups and the ν vibration of the carbonyl group of CONH [27]. Other major evolved gas products are CO_2 ($\bar{\nu} = 669 \text{ cm}^{-1}$ and 2349 cm^{-1}), CO, hydrocarbons and NH_3 (930, 965, 1626 and 3332 cm^{-1}). At 500 °C, mainly CO_2 and CO are released, and traces of ϵ -caprolactam and ammonia are also found.

For the PA6/GAS 5% formulation, at 320 °C, peaks corresponding to ammonia are already detected, whereas water is also observed with peaks around 3600 cm^{-1} and 1500 cm^{-1} . Compared to the spectra of the first degradation step of neat PA6, an additional double peak has appeared at $\bar{\nu} = 2070$ and 2045 cm^{-1} . This double peak was attributed, using the NIST (National Institute of Standards and Technology) database of infrared spectra [22], to $\text{C}\equiv\text{N}$ and/or $\text{C}-\text{C}\equiv\text{N}$ bonds. The formation of such compounds when PA6 degrades is already reported in the literature [28]. It could thus be assumed that GAS modifies the degradation pathway of PA6, leading to the formation of molecules presenting nitrile end-groups. For higher temperatures, there are no main differences comparing the spectra obtained for PA6/GAS with those of virgin PA6.

Concerning the PA6/GAS 2.5%/MPP 2.5% formulation, at 320 °C, CO_2 , NH_3 and water are released. At the maximum weight loss rate of the main degradation step (around 430 °C), the same gases (NH_3 , CO_2 , H_2O) are released along with CO and ϵ -caprolactam ($\bar{\nu} = 1,713$ and 2938 cm^{-1}). However, not only ϵ -caprolactam corresponds to these vibration bands, and other scission products of PA6 may appear within those wavenumbers. For such a heat treatment temperature, a low intensity peak corresponding to nitrile-ends at $\bar{\nu} = 2250 \text{ cm}^{-1}$ is also observed. During the last step, at 500 °C, mainly CO and CO_2 are released, and this step corresponds to the transient char oxidation.

3.4. Analysis of the Solid Phase

In order to go further into the investigation of the mode of action of MPP/GAS to flame retard PA6, the degradation products of the condensed phase were then analyzed to detect potential chemical reactions between PA6, GAS, MPP and/or their degradation products. Solid-state NMR was chosen to study the condensed phase.

The ^{13}C solid-state NMR spectra of the PA6/GAS 2.5%/MPP 2.5% at ambient temperature and treated at different characteristic temperatures are presented in Figure 7. The temperatures were selected according to the TG curves. Two hundred seventy degrees Celsius corresponds to the beginning of the first degradation step; 320 °C is the maximum weight loss rate of the first step; 410 °C is around the maximum weight loss rate of the second (main) step of degradation; 490 °C corresponds to the beginning of the oxidation of the transient residues. There is no change in the ^{13}C solid-state NMR spectra between 20 and 320 °C: the aliphatic carbons are detected in the range of 20 to 45 ppm, and the carbonyl group is located at 170 ppm. From 410 to 490 °C, the spectra change; namely, the $\text{C}=\text{O}$ peak disappears, and the aliphatic region broadens. At 490 °C, the aliphatic carbons have almost disappeared, and a broad band centered at 130 ppm can be distinguished, corresponding to unsaturated carbon bonds (*i.e.*, aromatic species). Because of the high temperature, oxidized aromatic carbons appear characterized by the shoulder observed between 150 and 160 ppm.

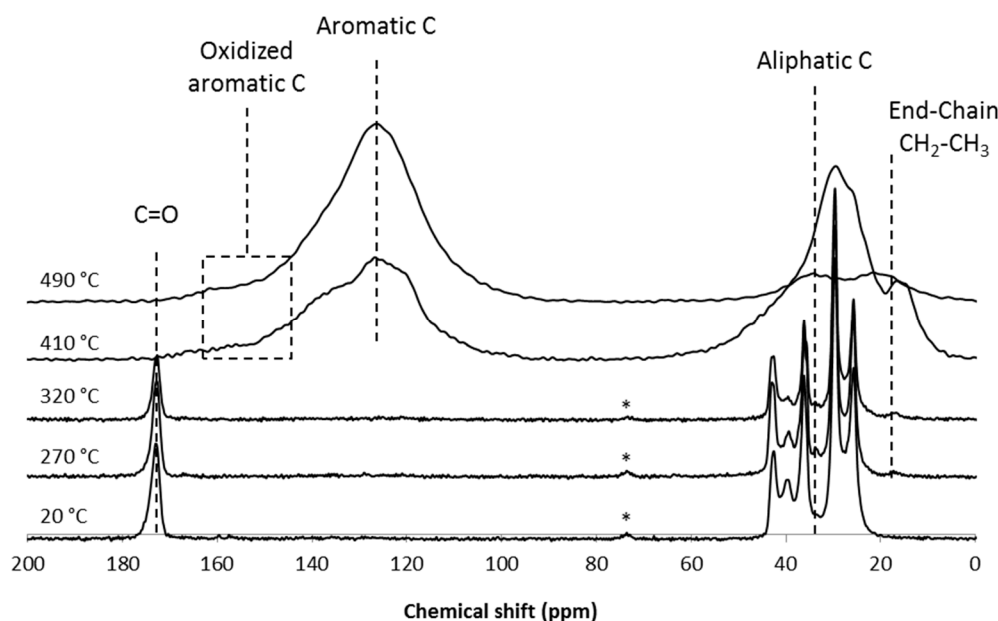


Figure 7. ^{13}C CP-DD-MAS NMR spectra of the PA6/GAS 2.5%/MPP2.5% residues obtained after thermal treatment at 20, 270, 320, 410 and 490 °C (* spinning sideband).

Additionally, ^{31}P solid-state NMR was performed on the formulation containing MPP. First, the NMR spectrum of pure MPP was recorded (Figure 8). It exhibits three main signals: a double peak at -21.5 and -24.2 ppm corresponding to linear polyphosphates; another peak at -11 ppm attributed to pyrophosphates; and eventually, at 0 ppm, a peak characteristic of H_3PO_4 . The other peaks correspond to spinning sidebands.

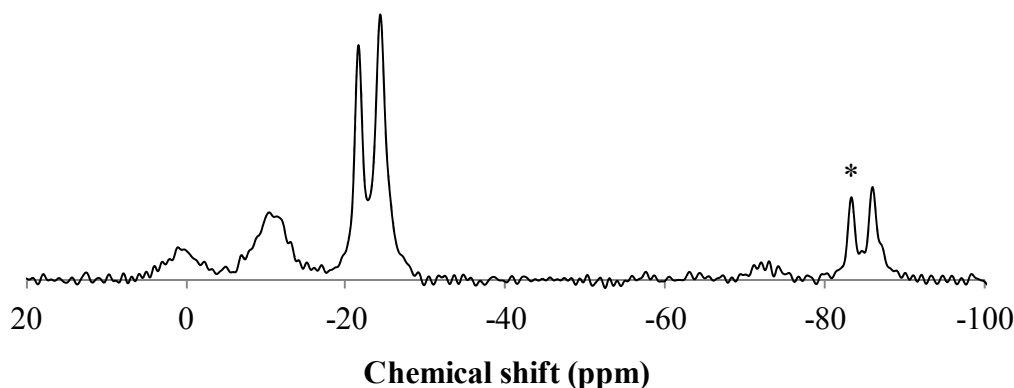


Figure 8. ^{31}P CP-high-power dipolar decoupling (HPDEC)-MAS NMR spectra of MPP (* spinning sideband).

The NMR experiments were done on the same thermally-treated samples as those used for ^{13}C NMR. The spectra are presented in Figure 9. It is possible to distinguish the three previously-described phosphate signals. For the ease of comprehension, the groups have been highlighted. At 20 °C, mainly polyphosphates are found, but a small amount of ortho and pyrophosphates are also detected. However, it has to be noted that the resolution of the spectra is lower than in the case of pure MPP. This thus demonstrates that the extrusion process affects, from some aspect, the structure (probably the crystallinity) of the MPP. At 270 °C, the spectrum is similar to that obtained at 20 °C, meaning that MPP is not or only

slightly degraded. This is consistent with the previously-reported data using TGA-FTIR. Indeed, it was demonstrated that the first degradation step starts at 270 °C, a temperature at which the weight loss is very low (around 1%). On the other hand, according to the work of Chen and Wang [29], pure melamine phosphate condenses on itself to form melamine pyrophosphate in the range of 260–300 °C, and these data are consistent with the obtained results, which show no depolymerized MPP at 270 °C. As the temperature continues to increase to 320 °C, the pyrophosphate peak becomes predominant, but the polyphosphate peak is still visible. It is thus assumed that MPP has started to degrade, but is not completely depolymerized. At higher temperatures (410 and 490 °C), the orthophosphate peak is the highest. However, particular attention should be paid to the attribution of the peaks. At 0 ppm, the peak can correspond not only to H_3PO_4 , but may also be attributed to $-\text{PO}_4$ units in R_2HPO_4 and RH_2PO_4 (with $\text{R} = \text{alkyl}$). At -11 ppm, the peak could also be attributed to $-\text{PO}_4$ units in $\varphi_2\text{RPO}_4$ (with $\varphi = \text{aromatic group}$) and/or $\varphi_2\text{HPO}_4$ and/or polyphosphate chain end-groups [30]. Since PA6 is a polymer that can contribute to carbonization, the formation of such species cannot be neglected. Moreover, since ^{13}C NMR shows the formation of a polyaromatic network at such a temperature, the formation of $\varphi_2\text{RPO}_4$ and/or $\varphi_2\text{HPO}_4$ makes sense at 410 and 490 °C.

As a conclusion, the analyses of the condensed phase as a function of temperature evidence the formation of a polyaromatic structure trapping phosphate-based molecules. Since MPP is well known as an intumescent additive [31], it could be used as an inorganic acid source. Upon heating, it produces, *in situ*, phosphoric acid, which catalyzes the char formation process, and melamine acts as a blowing agent. Such a phenomenon can be assumed in our case, even if, since the amount of MPP used in the formulation is low, this effect should not be preponderant, considering the flame retardant action of MPP/GAS.

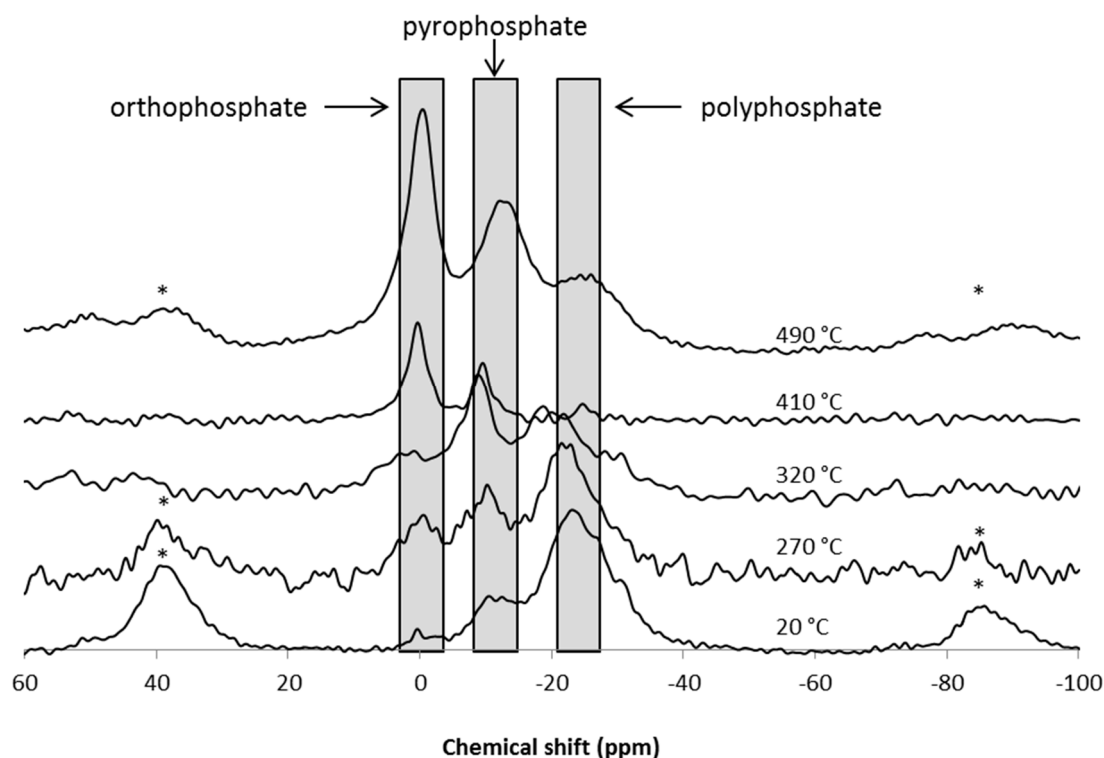


Figure 9. ^{31}P CP-HPDEC-MAS NMR spectra of the PA6/GAS 2.5%/MPP2.5% residues obtained after thermal treatment at 20, 270, 320, 410 and 490 °C (* spinning sideband).

4. Conclusions

The present work investigates the flame retardancy of PA6 using a combination of sulfur- and phosphorus-containing compounds. MPP was found to be an effective co-additive for GAS. Indeed, by varying the ratio of GAS/MPP and keeping a total FR loading of 5 wt%, the MCC results could be enhanced. For a formulation containing 5 wt% of MPP, a reduction of 10% of the pHRR is obtained; with 5 wt% of GAS, the pHRR is decreased by 15%; and finally, the combination GAS/MPP using a 50/50 ratio provides a further reduction to 30%, demonstrating an improvement of the performances combining P and S. This formulation was thus selected and then successfully extruded at the pilot scale.

Cone calorimetry does not show any improvement of the FR properties with this formulation, even though char formation occurs at the end of the experiment. TTI is significantly decreased compared with neat PA6. It is assumed that GAS and MPP promote PA6 degradation and consequently speed up fuel formation and release. Further tests have shown enhancements of the fire behavior: LOI jumps from 28 vol% for neat PA6 to 37 vol% for the PA6/GAS 2.5%/MPP 2.5% formulation, and the UL 94 classification is also improved and goes from V2 to V0. In both tests, it was proposed that higher dripping is responsible for the results. For LOI, the flame is removed from the burning zone by the heavy dripping, and the same phenomenon is observed in the UL 94 test; drips remove heat.

Analysis of the gas phase and of the condensed phase shows that GAS and MPP modify the degradation pathway of PA6 in a similar way as GAS does. For PA6, caprolactam was determined as the main degradation product. When GAS and MPP are added to the formulation, nitrile end-group molecules were found as degradation products of PA6. It is assumed that these compounds burn less efficiently, leading to an enhancement of the MCC results. On the other hand, GAS promotes char formation at high temperature, and the presence of MPP in the formulation enhances this process, as demonstrated by solid-state NMR. However, due to the low content of MPP in the formulation and/or its kinetics of formation, the char is not efficient enough to allow better performances in the cone calorimeter.

Acknowledgments

The authors want to thank the French National Research Agency for the financial support of this project (ArchiFlame: ANR- 2010-INTB-901-01).

Author Contributions

Sheng Zhang and Serge Bourbigot conceived and designed the experiments; Mathieu Coquelle and Jun Sun performed the experiments; Mathilde Casetta and Xiaoyu Gu analyzed the data; Sophie Duquesne wrote the paper.

Conflicts of Interest

The authors declare no conflict of interest.

References

1. Lewin, M.; Brozek, J.; Martens, M.M. The system polyamide/sulfamate/dipentaerythritol: Flame retardancy and chemical reactions. *Polym. Adv. Technol.* **2002**, *13*, 1091–1102.
2. Dahiya, J.B.; Kandola, B.K.; Sitpalan, A.; Horrocks, A.R. Effects of nanoparticles on the flame retardancy of the ammonium sulphamate-dipentaerythritol flame-retardant system in polyamide 6. *Polym. Adv. Technol.* **2013**, *24*, 398–406.
3. Coquelle, M.; Duquesne, S.; Casetta, M.; Sun, J.; Zhang, S.; Bourbigot, S. Investigation of the decomposition pathway of polyamide 6/ammonium sulfamate fibers. *Polym. Degrad. Stab.* **2014**, *106*, 150–157.
4. Sasaki, Y.; Suzuki, Y.; Fujimoto, T.; Miki, K. Jpn. patent 53133257. *Chem. Abstr.* **1978**, *90*, 105016w.
5. Yang, H.H. Polyamide fibers. In *Handbook of Fiber Chemistry*, 3rd ed.; Lewin, M., Ed.; CRC Press: Boca Raton, FL, USA, 2006; Volume 8.
6. Levchik, S.V.; Costa, L.; Camino, G. Effect of the fire-retardant, ammonium polyphosphate, on the thermal decomposition of aliphatic polyamides: Part II—Polyamide 6. *Polym. Degrad. Stab.* **1992**, *36*, 229–237.
7. Levchik, S.V.; Weil, E.D. Combustion and fire retardancy of aliphatic nylons. *Polym. Int.* **2000**, *49*, 1033–1073.
8. *Tests for Flammability of Plastic Materials for Parts in Devices and Appliances*; UL 94; Underwriters Laboratories Inc. (UL): Northbrook, IL, USA, 2001.
9. *Standard Test Method for Determining Flammability Characteristics of Plastics and Other Solid Materials Using Microscale Combustion Calorimetry*; ASTM D7309-07a; ASTM International: West Conshohocken, PA, USA, 2007.
10. International Organization for Standardization. *Plastics—Simple Heat Release Test Using a Conical Radiant Heater and a Thermopile Detector*; ISO 13927:2001; International Organization for Standardization: Geneva, Switzerland, 2001.
11. International Organization for Standardization. *Plastics—Determination of Burning Behaviour by Oxygen Index—Part 2: Ambient-Temperature Test*; ISO 4589-2:1996; International Organization for Standardization: Geneva, Switzerland, 1996.
12. Samyn, F.; Bourbigot, S.; Jama, C.; Bellayer, S. Fire retardancy of polymer clay nanocomposites: Is there an influence of the nanomorphology? *Polym. Degrad. Stab.* **2008**, *93*, 2019–2024.
13. Schartel, B.; Pawlowski, K.H.; Lyon, R.E. Pyrolysis combustion flow calorimeter: A tool to assess flame retarded PC/ABS materials? *Thermochim. Acta* **2007**, *462*, 1–14.
14. Morgan, A.B. Cone calorimeter and pyrolysis combustion flow calorimeter testing of polyurethane foams—A call for collaboration to establish a predictive model. In Proceedings of the 23rd Annual Conference on Recent Advances in Flame Retardancy of Polymeric Materials 2012, Stamford, CT, USA, 21–23 May 2012; pp. 254–266.
15. Lewin, M.; Zhang, J.; Pearce, E.; Gilman, J. Flammability of polyamide 6 using the sulfamate system and organo-layered silicate. *Polym. Adv. Technol.* **2007**, *18*, 737–745.
16. Schartel, B.; Pötschke, P.; Knoll, U.; Abdel-Goad, M. Fire behaviour of polyamide 6/multiwall carbon nanotube nanocomposites. *Eur. Polym. J.* **2005**, *41*, 1061–1070.

17. Samyn, F. *Compréhension des procédés d'ignifugation du polyamide 6*; Université Lille I: Lille, Nord, France, 2007. (In French)
18. Levchik, S.V.; Balabanovich, A.I.; Levchik, G.F.; Costa, L. Effect of melamine and its salts on combustion and thermal decomposition of polyamide 6. *Fire Mater.* **1997**, *21*, 75–83.
19. Kandola, B.K.; Price, D.; Milnes, G.J.; da Silva, A. Development of a novel experimental technique for quantitative study of melt dripping of thermoplastic polymers. *Polym. Degrad. Stab.* **2013**, *98*, 52–63.
20. Dupretz, R.; Fontaine, G.; Duquesne, S.; Bourbigot, S. Understanding of phenomena through instrumentation of UL-94 test. In Proceedings of Journée des Jeunes Chercheurs de l'UGéPE, Mons, Belgium, 23 October 2014.
21. Levchik, S.V.; Weil, E.D.; Lewin, M. Thermal decomposition of aliphatic nylons. *Polym. Int.* **1999**, *48*, 532–557.
22. Stein, S.E. Infrared Spectra. In *NIST Chemistry WebBook; NIST Standard Reference Database No. 69*; Linstrom, P.J., Mallard, W.G., Eds.; National Institute of Standards and Technology: Gaithersburg, MD, USA, 2001.
23. Seefeldt, H.; Duemichen, E.; Braun, U. Flame retardancy of glass fiber reinforced high temperature polyamide by use of aluminum diethylphosphinate: Thermal and thermo-oxidative effects. *Polym. Int.* **2013**, *62*, 1608–1616.
24. Pretsch, E.; Bühlmann, P.; Badertscher, M. IR Spectroscopy. In *Structure Determination of Organic Compounds: Tables of Spectral Data*, 4th ed.; Springer: Berlin, Germany, 2009.
25. Socrates, G. *Infrared and Raman Characteristic Group Frequencies: Tables and Charts*, 3rd ed.; Wiley: Hoboken, NJ, USA, 2004.
26. Fuller, M.P.; Griffiths, P.R. Infrared microsampling by diffuse reflectance fourier transform spectrometry. *Appl. Spectrosc.* **1980**, *34*, 533–539.
27. Pramoda, K.P.; Liu, T.; Liu, Z.; He, C.; Sue, H.J. Thermal degradation behavior of polyamide 6/clay nanocomposites. *Polym. Degrad. Stab.* **2003**, *81*, 47–56.
28. Davis, R.D.; Gilman, J.W.; VanderHart, D.L. Processing degradation of polyamide 6/montmorillonite clay nanocomposites and clay organic modifier. *Polym. Degrad. Stab.* **2003**, *79*, 111–121.
29. Chen, Y.; Wang, Q. Reaction of melamine phosphate with pentaerythritol and its products for flame retardation of polypropylene. *Polym. Adv. Technol.* **2007**, *18*, 587–600.
30. Bourbigot, S.; Bras, M.L.; Delobel, R. Carbonization mechanisms resulting from intumescence association with the ammonium polyphosphate-pentaerythritol fire retardant system. *Carbon* **1993**, *31*, 1219–1230.
31. Duquesne, S.; Fütterer, T. Intumescent Systems. In *The Non-halogenated Flame Retardant Handbook*; Morgan, A.B., Wilkie, C.A., Eds.; Wiley: Hoboken, NJ, USA, 2014; pp. 293–346.